ELSEVIER

Applied Surface Science 175–176 (2001) 49–54

applied surface science

www.elsevier.nl/locate/apsusc

Influence of the electrochemical potential on energy landscapes near step- and island-edges: Ag(100) and Ag(111)

Michael I. Haftel[a,b,*], Theodore L. Einstein[b]

[a]*Code 6331, Naval Research Laboratory, Nonstructure Optics Section, Washington, DC 20375-5343, USA*
[b]*Department of Physics, University of Maryland, College Park, MD 20742-4111, USA*

Accepted 2 January 2001

Abstract

The electrochemical cell offers the promise of enabling controlled alteration of the morphology and islanding phenomena on metallic surfaces. Different diffusion processes near step and island edges are known to profoundly affect the growth mode, island sizes, island shapes and step morphology. Using the surface-embedded-atom model (SEAM) modified for the electrolytic environment, we calculate the dependence of the activation energies for these diffusion processes on the electrochemical potential for the Ag(100) and Ag(111) surfaces. While all these processes show some degree of dependence on the potential, the step-edge barrier and the edge diffusion processes are the most sensitive. Step-edge barriers for Ag(111) increase (to over 1 eV) with a 1.0 V potential (relative to the potential of zero charge (PZC)). The variations for Ag(100) are not as large (about 0.3 eV), but the excess step-edge barrier can be negative for high positive ($>+0.6$ V) or negative (<-0.4 V) potentials owing to the competing roles of hopping and exchange diffusion processes and their dependencies on the potential. Edge diffusion decreases rapidly with potential for both (100) and (111) surfaces. Significant variations are also found for diffusion around corners and kinks, which play important roles in island morphology. We assess the influence these variations have on island sizes, shapes, diffusion, and coarsening. From this discussion, we show how the electrochemical potential can be used to control the fractal or compact nature of islands, and the magnitude and scaling exponent for island diffusion and coarsening.

PACS: 68.35Bs; 68.35.Fx; 68.55-a

Keywords: Diffusion barriers; Embedded-atom model; Electrochemical effects; Surface morphology

1. Introduction

Several recent investigations [1–4] have indicated that the early film growth and morphology of metal surfaces can be radically different in the electrochemical cell than in ultra-high vacuum (UHV). Moreover, these surface features can change over rather small changes in the applied electrochemical potential, as exhibited in the needle-like growth of Ni on Au(111) [2] and the low-index reconstructions of Pt(110) [3], Au(100) and Au(111) [4]. In light of the intense interest in controlling surface structure on the nanoscale, the possibility of exploiting the electrochemical environment, e.g., through the applied potential naturally presents itself.

* Corresponding author. Present address: Code 6331, Naval Research Laboratory, Nonstructure Optics Section, Washington, DC 20375-5343, USA. Tel./fax: +1-202-767-2961.
E-mail address: haftel@ccf.nrl.navy.mil (M.I. Haftel).

0169-4332/01/$ – see front matter
PII: S0169-4332(01)00158-1

Island and step morphology depend a great deal on kinetic as well as thermodynamic factors. Both types of properties can often be predicted from atomic-level calculations. A huge body of work exists on the atomistic prediction of surface energetics and kinetics in the UHV environment, but virtually nothing for the electrochemical environment. The main purpose of this paper is to apply such an atomistic approach, based on the embedded-atom model (EAM), to the investigation of the effect of the electrochemical potential on diffusion barriers at and near island- or step-edges, and further how changes in these barriers can influence islanding phenomena. We concentrate on the Ag(111) and Ag(100) surfaces as many experimental [5–8] and theoretical [9,10] studies on these surfaces have been carried out.

In this study, we employ the semiempirical surface-embedded-atom model (SEAM) [11] to calculate the energetics of single atoms migrating on Ag surfaces near steps, corners, and kinks. The SEAM yields realistic surface energies and migration energies on low-index Ag surfaces [12]. We review the modifications of the SEAM for surface charge in Section 2. The following sections will assess the influence of the electrolytic surface charge on kinetic barriers and then on island sizes, shapes, and coarsening kinetics.

2. Embedded-atom model of metal–electrolyte interface

The EAM expression for the total potential energy is given by [13]

$$E = \sum_{i<j} V_{ij}(r_{ij}) + \sum_i F_i(\rho_i), \tag{1a}$$

where in the absence of surface charge

$$\rho_{\mathrm{i}} = \sum_{j\neq i} \phi_j(r_{ij}), \tag{1b}$$

where V_{ij} is the pair potential, F_i the embedding function of atom i, ρ_i the electron density produced by all other atoms, and ϕ_j the electron density produced by atom j. In the SEAM [11] we fit the functions F, V, and ϕ to empirical surface and bulk properties of Ag.

We modify the SEAM to the charged environment [14,15] by simply adding an extra effective electron density $\Delta\rho_i$ determined by the excess charge deposited on the surface to the "background" electron density produced by all the other atoms, i.e.,

$$\rho_i = \sum_{j\neq i} \phi_j(r_{ij}) + \Delta\rho_i. \tag{2}$$

To relate the change in electron density at surface sites $\Delta\rho$ to the surface charge q (or its areal density σ), we assume that the surface charge is uniformly distributed over a height h at the surface

$$\Delta\rho = -\frac{\sigma}{h}. \tag{3}$$

The quantity h becomes a free parameter of our method, and it is determined by fitting the experimental capacitance in electrolytic solution (about 75 μF/cm^2). Details of the fitting procedure as well as the full description of the surface charge modified SEAM are given elsewhere [14–17]. While we fit parameters to electrolytic properties (capacitance and work functions) measured for (111) surfaces, the resulting potential accurately describes electrolytic properties on other surfaces as well (such as the PZC) leading us to conclude that our simple approach captures the essential physics of the surface charge. Once we can calculate the energy as a function of surface charge (or σ) we can calculate the potential ($\sim$dE/dq) and energy as a function of potential. We can also calculate other quantities such as the stress or the migration energy of a single adatom as functions of charge or potential.

3. Results — diffusion barriers

Table 1 contains the activation barriers for Ag(100) and Ag(111) for diffusion along the terrace, over the step-edge, along the step-edge, around corners and kinks, as well as detachment/attachment from the step-edge and (for (100)) from the kink along the step-edge. The difference between attachment and detachment comes from the additional binding to step-edge sites (compared to the open terrace) and kink sites (compared to the straight step-edge). The Ag (111) results are for the (100) microfaceted step-edge, and the corner here is a 60° corner. Results

Table 1
Diffusion barriers on terraces, over step-edges, and along step-edges and around corners and kinks[a]

	$\Delta\rho = -0.35$	$\Delta\rho = -0.15$	$\Delta\rho = 0.0$	$\Delta\rho = 0.10$	$\Delta\rho = 0.20$
Ag(100)					
$\Phi(q) - \Phi(0)$ (111)	701	231	−51	−216	−655
Surface stress	175	166	159	152	105
Terrace	*590*	*375*	*402*	*386*	301
Step-edge	*519*	*436*	*441*	*390*	*404*
Step-edge detach	*794*	*619*	*655*	*668*	843
Step-edge attach	*603*	*362*	*426*	385	458
Along step-edge	645	435	314	249	183
Around kink	*687*	*440*	*417*	*454*	484
Around corner	*543*	*399*	*507*	551	492
Detach from kink	802	653	563	510	441
Attach to kink	594	380	257	203	148
Ag(111)					
$\Phi(q) - \Phi(0)$ (111)	854	324	0	−543	−1108
Surface stress	146	178	200	158	98
Terrace	58	116	119	100	64
Step-edge	1217	*353*	*234*	*261*	*274*
Step-edge detach	787	686	641		561
Step-edge attach	49	72	74		17
Along step-edge	482	366	293	221	164
Around kink	597	477	400	334	323
Around corner	598	477	398	334	323

[a] Excess electron densities are relative to equilibrium bulk. Double layer potentials are in mV, surface stress in meV/Å^2. All diffusion energies are in meV. Italic figures indicate that exchange is favored over hopping diffusion. Diffusion energies are for a single adatom migrating over or along the stated feature. Detachment energies are for a single atom forming the described feature, while attachment energies are for an adatom attaching to the feature.

are given for five values of the electron density shift of Eq. (3), with the potential relative to the PZC of the (111) face (i.e., $\Phi(q) - \Phi(0)$ (111)) also given.

Large sensitivities to surface charge occur for most of the diffusion constants in Table 1. Generally, diffusion barriers rise with increasing positive charge or voltage, but there are counterexamples. Trends are not necessarily the same for (111) as for (100) (e.g., the terrace diffusion barriers on (100)), and often the preferred diffusion mechanism, hopping or exchange, may change with surface charge. The Ehrlich–Schwoebel (ES) excess step-edge barrier E_{ES}, the difference between the step-edge and terrace diffusion barriers, exhibits opposite trends for (100) and (111), being very large at high positive charge (negative $\Delta\rho$) for (111) and even becoming negative under the same conditions on (100). The analog ''kink'' excess barrier for diffusion along the step-edge is rather insensitive for (111), while increasing with negative charge on (100). As we have described previously, the diffusion energy trends are complicated, often nonmonotonic, because of the competing influences of stress [18] and bond counting on the diffusion energies for both hopping and exchange diffusion. The electrochemical ''tuning'' of these barriers, important in both 3D and 2D islanding, becomes a possibility.

How can the variation of diffusion barriers in Table 1 influence the size and shapes of 2D islands? Nucleation theory [19] tells us that the mean island size (in number of atoms) $\langle N \rangle \sim (D/F)^{i/(i+2)}$, where D is the terrace diffusion constant, F the incident deposition flux, and i the size of the largest mobile island. With $D = v_0 a^2 \exp(-E_{TD}/kT)$, where E_{TD} is the terrace diffusion barrier and v_0 the vibrational attempt frequency (which we always take generically as 10^{12} s^{-1}), and assuming $i = 1$, we follow Zhang

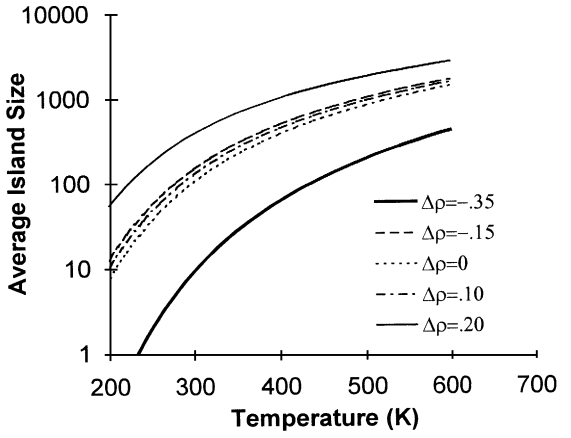

Fig. 1. Ag(100) island sizes using the terrace diffusion barriers of Table 1. The deposition rate is 0.2 ML/min, and the coverage is 0.25 ML.

et al. [20] to obtain

$$\langle N \rangle = \left(\frac{D\theta^2}{3Fa^4} \right)^{1/3}, \tag{4}$$

where θ is the coverage and a the nearest-neighbor spacing. Fig. 1 illustrates the temperature dependence of the average island size on Ag(100) for various surface charges under typical electrodeposition conditions. This figure indicates that one can have a large degree of control of the island size during a deposition phase by regulating the electrochemical potential: as it increases from -0.7 to $+0.7$ V relative to the PZC at room temperature, the average island size decreases from 500 to 10 atoms.

While terrace diffusion controls island size, the relative mobilities of atoms along the step-edge and on the terrace control the shape. If atoms can readily diffuse along the step-edge (typical of metal f.c.c. (100) surfaces), compact islands will result. If the edge atoms cannot diffuse very far before another one arrives from the terrace, the arriving atoms will "hit and stick", giving rise to fractal shapes. Zhang et al. have quantified the fractal-compact transition in terms of a ratio t_r/t_a, the ratio of residence time t_r an edge atom spends on a given edge of an island to the arrival time t_a of atoms diffusing from the terrace. A ratio $t_r/t_a < 1$ indicates a compact shape, while $t_r/t_a > 1$ indicates a fractal shape. Zhang et al. [20] importantly note that t_r depends on more than the edge

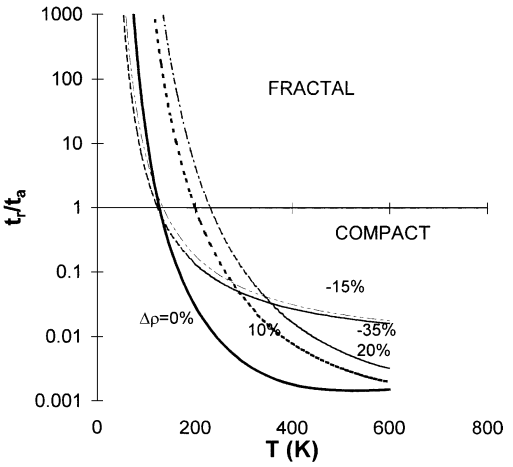

Fig. 2. Ratio of residence time on step-edge to arrival time of atoms from terrace for Ag(100). The coverage is $\theta = 0.1$ ML, and the island size is fixed at 500 atoms. Islands are fractal (compact) when the ratio is above (below) unity; the transition temperature is at the intercept.

diffusion: the corner-rounding barrier must also be taken into account in calculating t_r, which typically increases this residence time.

Figs. 2 and 3 give t_r/t_a as functions of temperature for Ag(100) and Ag(111), respectively. We utilize the expressions of Zhang et al. [20] for t_r and t_a, and the SEAM diffusion barriers for terrace diffusion, edge

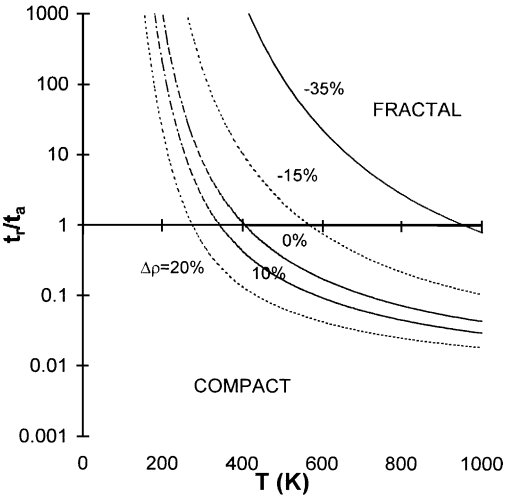

Fig. 3. Ratio of residence time on step-edge to arrival time of atoms from terrace for Ag(111) for the same conditions as for Ag(100) in Fig. 2.

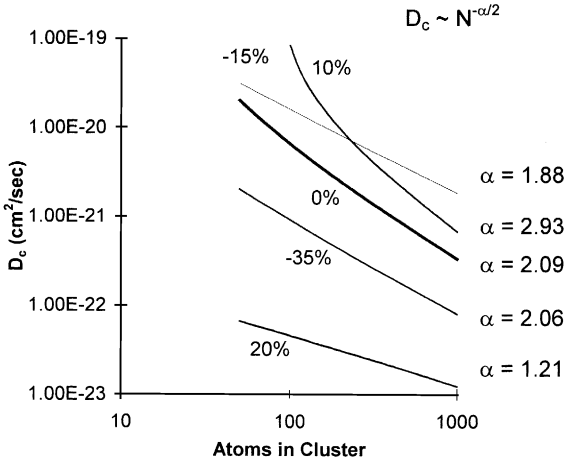

Fig. 4. Cluster diffusion constants at 300 K on Ag(100). The periphery diffusion barrier of [21] is determined by the SEAM-edge diffusion barrier. The scaling exponent α, evaluated at $N = 300$, is indicated for each curve.

diffusion, and corner diffusion, and the deposition flux F is adjusted to produce a mean island size of 500 atoms for $\theta = 0.1$ ML. While islands on Ag(100) are compact at room temperature (RT) in all cases, the transition temperature to a fractal shape varies from 130 to 230 K depending on surface charge. While the temperature trend is not strictly monotonic with charge, the largest negative and positive surface charges give the highest and lowest transition temperatures, respectively. The Ag(111) variations are much more dramatic than for Ag(100), with the opposite trend. The transition temperature varies from 250 to 960 K with the largest negative surface charge yielding the lowest transition temperature. The trend here is monotonic with surface charge. Though the Ag(111) islands are typically fractal at RT, applying a large enough negative potential $(\Phi - \Phi(0) - 0.5\,\mathrm{V})$ can produce compact islands instead.

In the late post-deposition phase, the islands diffuse and coarsen. The diffusion constant scales according to $D \sim N^{-\alpha/2}$. The islands coarsen according to $\langle N \rangle \sim t^{2\beta}$, where $\beta = 1/(\alpha + 2)$. Khare and Einstein [21] give the diffusion constants and scaling exponents in terms of the underlying diffusion constants. Using these expressions and the SEAM diffusion barriers, we obtain the cluster diffusion constants on Ag(100) depicted in Fig. 4. Again, there is a large variation in the magnitude and scaling of the diffusion constant with surface charge. The variation of these quantities with charge reflects the nonmonotonic nature of many of the diffusion constants and the intricate interplay of these constants in accounting for the cluster diffusion properties. Fig. 4 suggests that the electrochemical potential can be used powerfully to control the island coarsening dynamics.

4. Conclusions

Adatom diffusion constants, both on the flat terrace and over or near step-edges, are very sensitive to the surface charge deposited at potentials readily obtainable in electrochemical experiments. The diffusion barriers often exhibit complicated nonmonotonic behavior with the surface charge, more so on Ag(100) than on Ag(111), and results from the different effects of bond strength, surface stress, and the transitions between hopping and exchange diffusion as functions of the surface charge. The large variations in diffusion barriers translate into large variations in island size, shape, and island diffusion and coarsening properties. Thus, it appears that the electrochemical potential can be used to control these islanding characteristics, both in the deposition and post-deposition phases, to fabricate desired features on the nanoscale.

Acknowledgements

Support by The Office of Naval Research and the NSF-funded MRSEC at the University of Maryland is gratefully acknowledged.

References

[1] S.G. Corcoran, G.S. Chakarova, K. Sieradzki, Phys. Rev. Lett. 71 (1993) 1585.
[2] F.A. Möller, O.M. Magnussen, R.J. Behm, Phys. Rev. Lett. 77 (1996) 3165.
[3] C.A. Lucas, N.M. Markovic, P.N. Ross, Phys. Rev. Lett. 77 (1996) 4922.
[4] D.M. Kolb, Prog. Surf. Sci. 51 (1996) 109.
[5] J.M. Wen, S.L. Chang, J.W. Burnett, J.W. Evans, P.A. Thiel, Phys. Rev. Lett. 73 (1994) 2591.
[6] W.W. Pai, A.K. Swan, Z. Zhang, J.F. Wendelken, Phys. Rev. Lett. 79 (1997) 3210.
[7] C.R. Stoldt, C.J. Jenks, P.A. Thiel, A.M. Cadilhe, J.W. Evans, J. Chem. Phys. 111 (1999) 5157.

[8] H. Brune, H. Röder, C. Boragno, K. Kern, Phys. Rev. Lett. 73 (1994) 1955.
[9] J. Heinonen, I. Koponen, J. Merikoski, T. Ala-Nissila, Phys. Rev. Lett. 82 (1999) 2733.
[10] S. Pal, K.A. Fichthorn, Phys. Rev. B 60 (1999) 7804.
[11] M.I. Haftel, M. Rosen, Phys. Rev. B 51 (1995) 4426.
[12] M.I. Haftel, M. Rosen, Surf. Sci. 407 (1998) 16.
[13] M.S. Daw, M.I. Baskes, Phys. Rev. B 29 (1984) 6443.
[14] M.I. Haftel, M. Rosen, S.G. Corcoran, Mater. Res. Soc. Symp. 451 (1997) 31.
[15] M.I. Haftel, T.L. Einstein, Mater. Res. Soc. Symp. 580 (2000) 195.
[16] M.I. Haftel, M. Rosen, in preparation.
[17] M.I. Haftel, M. Rosen, Bull. Am. Phys. Soc. 44 (1999) 1831.
[18] B.D. Yu, M. Scheffler, Phys. Rev. B 56 (1997) R15569.
[19] J.G. Amar, F. Family, P.-M. Lam, Phys. Rev. B 50 (1994) 8781.
[20] T. Zhang, J. Zhong, Z. Zhang, M.G. Lagally, Preprint, 1999.
[21] S.V. Khare, T.L. Einstein, Phys. Rev. B 54 (1996) 11752.